



Antioxidant and Cardioprotective Evaluation of Some *N*-(3-Chloro-2-oxo-4-arylazetidin-1-yl)-2-[(4-oxo-2-aryl-4*H*-chromen-7-yl)oxy]acetamide Derivatives

DURBHAKA S. PADMINI^{1,*}, DUGASANI SWARNALATHA² and S.V.U.M. PRASAD³

¹Department of Pharmaceutical Chemistry, Creative Educational Society's College of Pharmacy, Chinnatekuru, Kurnool-518218, India

²Department of Pharmacognosy and Phytochemistry, Annamacharya College of Pharmacy, Newboinapalli, Rajampeta-516126, India

³School of Pharmaceutical Sciences, Jawaharlal Nehru Technological University Kakinada, Kakinada-53303, India

*Corresponding author: E-mail: dspadmini.pharma@gmail.com

Received: 26 July 2021;

Accepted: 15 September 2021;

Published online: 16 December 2021;

AJC-20623

A series of *N*-(3-chloro-2-oxo-4-arylazetidin-1-yl)-2-[(4-oxo-2-aryl-4*H*-chromen-7-yl)oxy]acetamide derivatives [SLP VI 1(a-d)-2(a-d)] were synthesized from 7-hydroxy flavone derivatives through the intermediate Schiff bases. The synthesized compounds were investigated for *in vitro* antioxidant property by DPPH radical scavenging assay. The title compounds with good antioxidant potency were further evaluated for possible cardioprotective effect by doxorubicin induced cardiotoxicity. All biochemical changes were normalized after oral administration of the test compounds at the dose of 50 µg/kg. The results showed the significant ($p < 0.05$) increase in antioxidant enzymes catalase and superoxide dismutase in heart tissue homogenates. These observations enable us to conclude that the synthesized derivatives SLP VI 1b, VI 1c, VI 2b and VI 2d have cardioprotective activity against doxorubicin induced cardiotoxicity. Further, an attempt has been made to perform *in silico* studies on the synthesized compounds to predict the interaction between test ligands and prospective cardiovascular protein targets using molecular docking tools. The title compounds have good binding affinity with MAPkinase P38 and PKCβ cardiovascular targets.

Keywords: Flavone, 2-Azetidinone, Antioxidant, Cardioprotective, Molecular docking.

INTRODUCTION

Recent data have shown the abnormal production of free radicals directly or indirectly associated with changes in molecular pathways, activation of growth factors that underpin the genesis of cardiac hypertrophy [1]. In a study, Ang II increases ROS production by potentiating of Nox2, which in turn stimulates the expression of WNT1 inducible signaling pathway protein [2]. Various experimental and clinical studies indicate oxidative stress seems to have a key role during the transition from compensated hypertrophy to heart failure [3].

Reactive oxygen species (ROS) contribute to cardiac fibrosis, which is among the most important structural and functional changes occurring in various heart diseases. Apart from the indirect effect on cardiac contractility, it has been reported that ROS could directly enhance the positive inotropic effect of compounds possibly by activation of ERK1/2 redox signalling pathways [4]. ROS could oxidize the myofibrillar proteins, resulting in contractile dysfunction observed in heart

failure [5,6]. Furthermore, ROS also seem to play a major role in the formation of oxidized LDL, an initial step in atherosclerosis, progression of the coronary artery disease and activation of matrix metalloproteinases leading in plaque rupture. Oxidative stress can set the acute myocardial infarction and it could also contribute to molecular and structural abnormalities observed after myocardial infarction. The data presented above and perusal of literature indicate that so far, an extensive effort has been put in the search for a remarkable link between cardiovascular diseases (CVD) and the impact of oxidative stress.

The greatest disadvantage of presently available and prescribed drugs lies in their adverse effects including reappearance of symptoms after discontinuation. Further, management of cancer chemotherapy induced toxicity is also challenging for researchers. Among several approaches, lessening the free radical generation and associated cardiotoxicity with use of natural antioxidants is the one of the best and most sought after approach. Nature has produced wonderfully complex molecules that no synthetic chemist could ever dream up [7] but

drug discovery from nature is far from straightforward. Several natural products like flavonoids, their semi-synthetic and synthetic analogues have been reported to exhibit multi-farious biological activities [8], of them, antioxidant activity remained a principle subject [9]. The most important features of flavonoids include their ability to protect against oxidative diseases, activate or inhibit various enzymes bind specific receptors and protect against cardiovascular diseases by reducing the oxidation of low-density lipoproteins. The extensive availability of literature evidenced that 2-azetidinones have antioxidant [10] effect apart from the antimicrobial, anti-inflammatory, anticancer and other potent biological activities [11-13].

Therefore an attempt was made on the rational development of new antioxidant molecules by tethering the active flavones with various 2-azetidinones. The newly synthesized potent antioxidant derivatives were explored further for cardio-protective effect. To extend our research, we use drug design approaches to find the drug-likeness, interaction between the synthesized compounds and cardiovascular targets using molecular docking tools.

EXPERIMENTAL

The synthesized molecules were characterized by physical and spectral techniques. The melting points of synthesized compounds were determined by open capillary tube method and are uncorrected. The progress of reaction and purity of products was checked by TLC, Merck silica gel plate (0.25 mm) and visualization by fluorescence quenching under UV light (254 nm). IR spectrum was taken on Fourier transform IR spectrophotometer (model Shimadzu 8400S) using KBr pellet technique. ¹H NMR spectra were recorded on Varian 400 MHz NMR spectrometer in DMSO solvent. Mass spectra were recorded on Agilent MS ion trap systems. The other instruments include Semi Auto analyzer (Maxlyzer, Avecon model no: NB-201), UV-visible spectrophotometer, electronic tissue homogenizer (Ever shine, Model no: 607), Remi centrifuge (Remi, Model no: KKLO-9013) were used for the study. CK-MB, LDH, AST, ALT, ALP and triglyceride estimation kits for cardioprotective evaluation were obtained from Erba kits, Delhi, India.

General procedure for the synthesis of chalcones [SLP I (1-2)]: To a mixture of aromatic aldehyde (1 mmol) and 2,4-dihydroxy acetophenone (1 mmol) in ethanol, a solution of KOH (2.5 mmol) in 20 mL of ethanol was added. The resulting mixture stirred with magnetic stirrer for 4 h and poured in to crushed ice and acidified with conc. HCl. The separated pale yellow solid mass was filtered, washed with ice cold water and recrystallized with hot ethanol to afford various 2',4'-chalconediols [SLP I (1-2)] (Scheme-I).

(2E)-1-(2,4-Dihydroxyphenyl)-3-(4-methoxyphenyl)-prop-2-en-1-one [SLP I 1]: Pale brownish yellow solid; m.p. 82-84 °C; yield: 68%; IR (KBr, ν_{\max} , cm^{-1}): 3420.54 (-OH *str.*), 1675.30 (C=O *str.*), 1634.65 (C=C *str.*), 2924.64 (-OCH₃ *str.*); ¹H NMR: δ 3.72 (s, 3H, -OCH₃), δ 12.79, 12.6 (s, 2H, Ar-OH), δ 6.97 (d, 2H, -COCH=CH-), δ 7.47 (M, 7H, Ar-H).

(2E)-1-(2,4-dihydroxyphenyl)-3-(4-(dimethylamino)-phenyl)prop-2-en-1-one [SLP I 2]: Reddish yellow solid; m.p.: 116 °C; yield: 67%; IR (KBr, ν_{\max} , cm^{-1}): 1676.81 (C=O

str.), 1638.53 (C=C *str.*), 3415.22 (-OH *str.*), 1250-1300 (C-N *str.*), 1434 (C-N bend), ¹H NMR: δ 6.84 (d, 1H, -CO-CH=CH-), δ 6.79 (d, 1H, -CO-CH=CH-), δ 7.4-7.7 (m, 5H, Ar-H), δ 12.1-12.7 (s, 4H, Ar-OH), 3.15 (s, 6H, -N (CH₃)₂).

General procedure for the synthesis of flavones [SLP II 1-2]: Chalcone [SLP I 1-2] (1 mmol) added with catalytic amount of I₂ (0.1 mmol) in DMSO and refluxed for 20-40 min, after dilution with excess of cold water the product was filtered, washed with 20% sodium thiosulphate solution to remove the colour of iodine to yield flavones [SLP II 1-2] (Scheme-I).

7-Hydroxy-2-(4-methoxyphenyl)-4H-1-benzopyran-4-one [SLP II 1]: Yellow solid; m.p.: 117 °C; yield: 60%; IR (KBr, ν_{\max} , cm^{-1}): 1636.30 (C=O *str.*), 1610 (C=C *str.*), 2924.36 (-OCH₃ *str.*), 1130.52 (C-O-C *str.*), 3423.90 (-OH *str.*); ¹H NMR: δ 3.9 (s, 3H, Ar-O-CH₃), δ 6.92 (s, 1H, -CO-CH=C<), δ 6.94-7.92 (m, 7H, Ar-H), δ 12.50 (s, 1H, C₇-OH).

2-[4-(Dimethylamino)phenyl]-7-hydroxy-4H-1-benzopyran-4-one [SLP II 2]: Pale yellow solid; m.p.: 128 °C; yield: 65%; IR (KBr, ν_{\max} , cm^{-1}): 1630.99 (C=O *str.*), 1191.83 (C-O-C *str.*) 3390.22 (-OH *str.*), 2855.32 (N-CH₃ *str.*), 2925.16 (C-H stret aromatic); ¹H NMR: δ 6.96 (m, 7H, Ar-H), δ 6.76 (s, 1H, -CO-CH=C<), δ 12.5 (s, 1H, C₇-OH), 3.22 (s, 6H, -N (CH₃)₂).

General procedure for synthesis of ethyl 2-[(4-oxo-2-aryledene-4H-chromen-7-yl)oxy]acetate [SLP III 1-2]: A flavone [SLP II 1-2] (0.01 mol) was dissolved in dry acetone (50 mL) and a solution of ethylchloroacetate (1.22 mL, 0.01 mol) was added. To this mixture, 0.4 g of anhydrous potassium carbonate was added. The resulting mixture was refluxed on water bath for 6 h. The solution was evaporated to dryness and the residue was washed with ethanol (50 mL), filtered and recrystallized from methanol to give the desired crystalline product (Scheme-I).

Ethyl 2-[(4-oxo-2-(4-methoxy phenyl)-4H-chromen-7-yl)oxy]acetate [SLP III 1]: Pale yellow solid, m.p. 128 °C; yield: 58%; IR (KBr, ν_{\max} , cm^{-1}): 1645.10 (C=O *str.*), 1743.03 (-C=O *str.* ester), 1658.67 (C=C *str.*), 3070.46 (-OCH₃ *str.*), 1132.14 (C-O-C *str.*); 1244.00 (C-O-C *str.* ester), 2893.02, 829.38, 2781.16, (-CH₂, -CH₃); ¹H NMR: δ 3.9 (s, 3H, Ar-O-CH₃), δ 6.95 (s, 1H, -CO-CH=C<), δ 6.94-7.92 (m, 6H, Ar-H), δ 1.18 (t, 3H, -COOCH₂CH₃), δ 4.10 (q, 2H, COOCH₂CH₃), δ 4.44 (s, 2H, -OCH₂-).

Ethyl 2-[(4-oxo-2-(4-dimethylaminophenyl)-4H-chromen-7-yl)oxy]acetate [SLP III 2]: yellow solid; m.p.: 109 °C; yield: 68%; IR (KBr, ν_{\max} , cm^{-1}): 1643.95 (C=O *str.*), 1757.68 (-C=O *str.* ester), 1662.69 (C=C *str.*), 1136.71 (C-O-C *str.*), 1236.81 (C-O-C *str.* ester), 2924.07, 2862.57, 2753.90, 1442.62 (-CH₂, -CH₃ *str.*).

General procedure for synthesis of 2-[(4-oxo-2-aryl-4H-1-benzopyran-7-yl)oxy]aceto hydrazides [SLP IV 1-2]: Ethyl 2-[(4-oxo-2-aryledene-4H-chromen-7-yl)oxy]acetate [SLP III 1-2] (0.01 mol) was taken in round bottom flask and hydrazine hydrate (0.01 mol, 0.9 mL) was added to it. To this reaction mixture, 1,4-dioxane (50 mL) was added and refluxed for 5 h maintaining the temperature 60-70 °C. Dark yellow coloured solid mass had appeared which was filtered, dried and recrystallized with ethanol to gain yellow crystalline product (Scheme-I).

2-[(4-Oxo-2(4-methoxy phenyl)-4*H*-1-benzopyran-7-yl)oxy]acetohydrazide [SLP IV 1]: Pale yellow solid, m.p.: 168 °C; yield: 65%; IR (KBr, ν_{\max} , cm^{-1}): 1649.49 (C=O *str.*), 1685.71 (-C=O *str.* amide), 2996.75, 2854.79 (-CH *str.*), 1172.76 (C-O-C *str.*), 3400.21, 3319.05, 3105.17 (N-H *str.*); $^1\text{H NMR}$: δ 3.88 (s, 3H, Ar-O-CH₃), δ 6.95 (s, 1H, -CO-CH=C<), δ 6.90-7.91 (m, 6H, Ar-H), δ 4.44 (s, 2H, -OCH₂-), δ 3.41 (s, 2H, -NH₂), δ 8.10 (s, 1H, -CONH).

2-[(4-Oxo-2(4-dimethylaminophenyl)-4*H*-1-benzopyran-7-yl)oxy]acetohydrazides [SLP IV 2]: Yellow solid; m.p.: 169 °C; yield: 70%; 1641.18 (C=O *str.*), 1690.85 (-C=O *str.* amide), 2928.13, 2842.48 (-CH *str.*), 1162.50 (C-O-C *str.*), 3401.40, 3313.50, 3118.60 (N-H *str.*).

General procedure for the synthesis of 2-[(4-oxo-2-aryl-4*H*-1-benzopyran-7-yl)oxy]-*N'*-[(*E*)-arylmethylidene]-acetohydrazides [SLP V 1(a-d)–2(a-d)] (Schiff bases): 2-[(4-Oxo-2-aryl-4*H*-1-benzopyran-7-yl)oxy]acetohydrazides [SLP IV 1-2] (0.01 mol, 2.91 g) and 30 mL methanol were taken in round bottom flask. Aromatic aldehyde was dissolved in 30 mL methanol and added slowly for about 20 min with vigorous stirring, maintaining the temperature at 40-50 °C. Four drops of glacial acetic acid was added and allowed to reflux for further 3 h at 40 °C. The mixture was poured into 250 mL ice-cold water and stirred. The precipitate obtained was filtered, dried and recrystallized from methanol. Pale yellow coloured solids (**Scheme-I**).

SLP V 1a: C₂₆H₂₂N₂O₆, yellow solid, m.p.: 245 °C; yield: 60%; IR (KBr, ν_{\max} , cm^{-1}): 1695.18 (-C=O *str.* amide), 1665.21 (C=N *str.*), 1645.22 (C=O *str.*), 1571.99 (C=C *str.*), 2925.95 (-OCH₃ *str.*), 2850.52 (C-H *str.*), 1134.07, (C-O-C *str.*), 1205.14 (C-N *str.*), 3371.18 (N-H *str.*), 3079.18 (=C-H *str.*); $^1\text{H NMR}$: δ 3.80 (s, 6H, Ar-O-CH₃), δ 6.95 (s, 1H, -CO-CH=C<), δ 4.40 (s, 2H, -OCH₂-), δ 6.5-7.9 (m, 11H, Ar-H), 8.92 (s, 1H, -CONH), δ 4.1 (s, 1H, -N=CH-).

SLP V 1b: C₂₆H₂₂N₂O₇, yellow solid, m.p.: 242 °C; yield: 61%; IR (KBr, ν_{\max} , cm^{-1}): 3529.52 (-OH *str.*), 1695.23 (-C=O *str.* amide), 1679.21 (C=N *str.*), 1628.01 (C=O *str.*), 1577.66 (C=C *str.*), 2931.60 (-OCH₃ *str.*), 2883.38, 2827.45 (C-H *str.*), 1128.12 (C-O-C *str.*); 1251.72 (C-N *str.*), 3318.77 (N-H *str.*), 3031.95 (=C-H *str.*); $^1\text{H NMR}$: δ 3.71 (s, 6H, Ar-O-CH₃), δ 12.2 (s, 1H, -OH), δ 6.9 (s, 1H, -CO-CH=C<), δ 4.42 (s, 2H, -OCH₂-), δ 6.5-8.2 (m, 10H, Ar-H), 8.92 (s, 1H, -CONH), δ 4.1 (s, 1H, -N=CH-).

SLP V 1c: C₂₇H₂₅N₃O₅, pale yellow solid, m.p.: 268 °C; yield: 50%; IR (KBr, ν_{\max} , cm^{-1}): 1697.95 (-C=O *str.* amide), 1664.45 (C=N *str.*), 1627.24 (C=O *str.*), 1598.88 (C=C *str.*), 2991.33 (-OCH₃ *str.*), 2816.88 (C-H *str.*), 2794.02, 2788.66, 2715.26 (N-CH₃ *str.*), 1137.20 (C-O-C *str.*); 1232.43 (C-N *str.*), 3177.97 (N-H *str.*), 3072.39 (=C-H *str.*), 1371.29 (CH₃ bend).

SLP V 1d: C₂₅H₁₈N₂O₅Cl₂, pale yellow solid, m.p.: 256-258 °C; yield: 68%; IR (KBr, ν_{\max} , cm^{-1}): 1696.71 (-C=O *str.* amide), 1659.34 (C=N *str.*), 1635.19 (C=O *str.*), 1601.39 (C=C *str.*), 2985.39 (-OCH₃ *str.*), 2810.48 (C-H *str.*), 1116.31 (C-O-C *str.*), 1238.66 (C-N *str.*), 3147.35 (N-H *str.*), 3099.09 (=C-H *str.*).

SLP V 2a: C₂₇H₂₅N₃O₅, yellow solid; m.p.: 151 °C; yield: 67%; IR (KBr, ν_{\max} , cm^{-1}): 1638.31 (C=N *str.*), 1672.89 (C=O

str.), 1672.90 (-C=O *str.* amide), 1646.12 (C=C *str.*), 1138.50 (C-O-C *str.*), 1229.81 (C-N *str.*), 3347.65 (N-H *str.*).

SLP V 2b: C₂₇H₂₅N₃O₆, yellow solid; m.p.: 169 °C; yield: 79%; IR (KBr, ν_{\max} , cm^{-1}): 3453 (-OH *str.*), 1642 (C=N *str.*), 1676 (C=O *str.*), 1673 (-C=O *str.* amide), 1642 (C=C *str.*), 1138.64 (C-O-C *str.*), 1231 (C-N *str.*); 3329 (N-H *str.*); $^1\text{H NMR}$: δ 3.9 (s, 3H, Ar-O-CH₃), δ 12.5 (s, 1H, -OH), 3.18 (s, 6H, -N(CH₃)₂), δ 6.92 (s, 1H, -CO-CH=C<), δ 6.94-7.92 (m, 10H, Ar-H), δ 4.41 (s, 2H, -OCH₂-), δ 8.3 (s, 1H, -CONH), δ 4.1 (s, 1H, -N=CH-).

SLP V 2c: C₂₈H₂₈N₄O₄, yellow solid; m.p.: 221 °C; yield: 70%; IR (KBr, ν_{\max} , cm^{-1}): 1641.11 (C=N *str.*), 1680.79 (C=O *str.*), 1667.88 (-C=O *str.* amide), 1640.21 (C=C *str.*), 1131.27 (C-O-C *str.*), 1239.48 (C-N *str.*), 3322.58 (N-H *str.*).

SLP V 2d: C₂₆H₂₁Cl₂N₃O₄, pale yellow solid; m.p.: 208-210 °C; yield: 62%; IR (KBr, ν_{\max} , cm^{-1}): 1647.73 (C=N *str.*), 1688.94 (C=O *str.*), 1671.63 (-C=O *str.* amide), 1640.90 (C=C *str.*), 1126.11 (C-O-C *str.*), 1228.56 (C-N *str.*), 3301.72 (N-H *str.*), 690-720 (C-Cl *str.*).

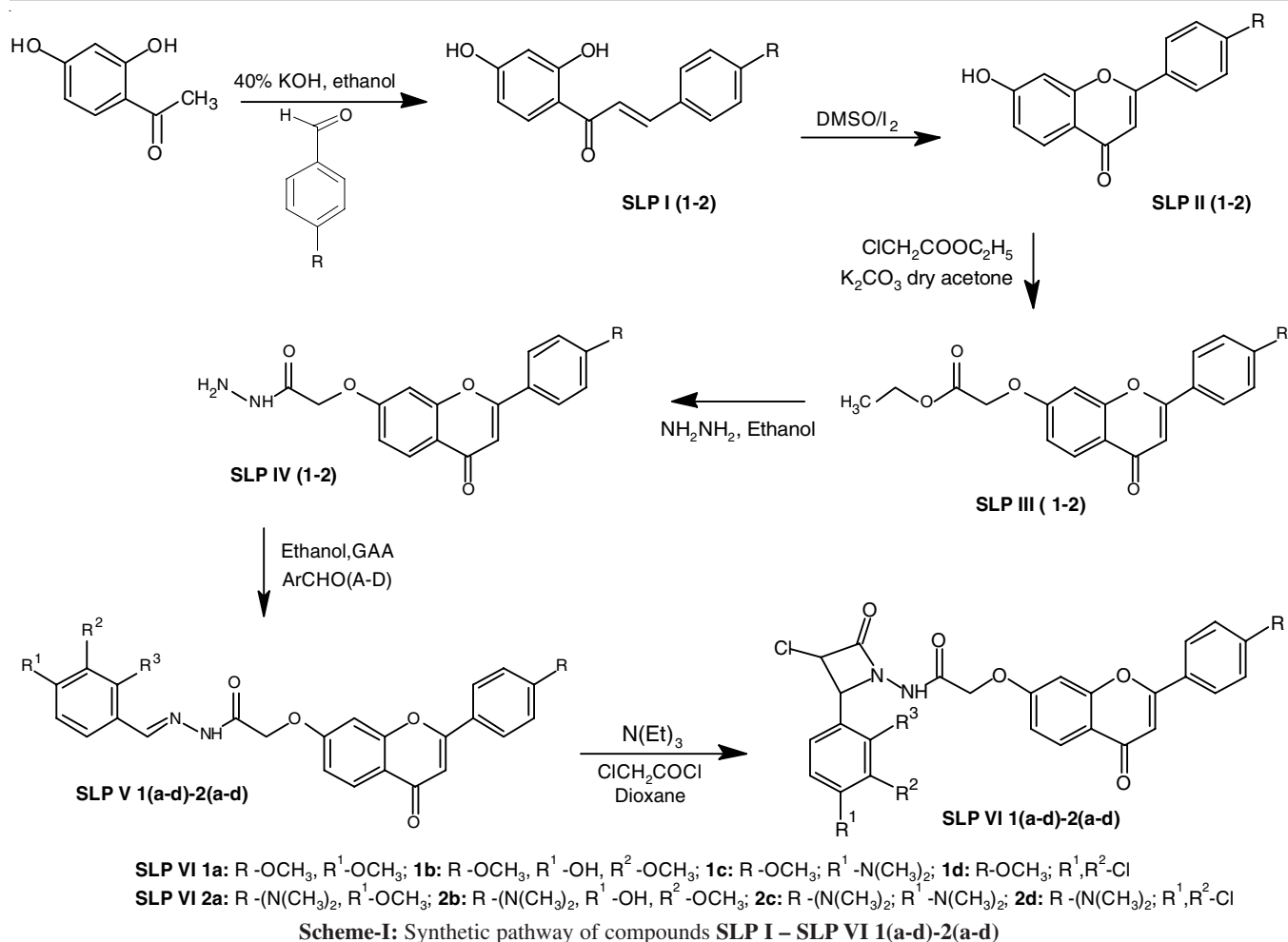
Procedure for synthesis of *N*-(3-chloro-2-oxo-4-arylazetid-1-yl)-2-[(4-oxo-2-aryl-4*H*-chromen-7-yl)oxy]-acetamide SLP VI [1(a-d)–2(a-d)]: A solution of chloroacetyl chloride (1.12 mL 0.01 M) in 1,4-dioxane was added dropwise to a well stirred solution of 2-[(4-oxo-2-aryl-4*H*-1-benzopyran-7-yl)oxy]-*N'*-[(*E*)-aryl methylidene]acetohydrazides [SLP V [1(a-d)–2(a-d)]] [Schiff bases] (0.01 M) and triethylamine (0.02 M) in 1,4-dioxane. After the addition had been completed, the solution was stirred for 24 h. The reaction mixture was added to ice cold water. The separated solid was filtered and purified from 1,4-dioxane:water (80:20) (**Scheme-I**).

SLP VI 1a: C₂₈H₂₃N₂O₇Cl, m.p.: 182-184 °C; yield: 62%. R_f: 0.608; benzene:acetone (7:3); IR (KBr, ν_{\max} , cm^{-1}): 1662.74 (C=O *str.*), 1744.60 (C=O *str.*), 696.55 (C-Cl *str.*), 1260 (N-N *str.*), 1610 (C=C *str.*), 2980 (-OCH₃ *str.*), 1125 (C-OC *str.*); 1191 (C-N *str.*); $^1\text{H NMR}$: δ 3.80 (s, 6H, Ar-O-CH₃), 6.95 (s, 1H, -CO-CH=C<), 4.40 (s, 2H, -OCH₂-), 6.5-7.9 (m, 11H, Ar-H), 8.92 (s, 1H, -CONH), 5.95 (s, 1H, -N-CH-ph), 4.63 (s, 1H, -CH-Cl). MS(EI, *m/z*): 535 (M+H⁺).

SLP VI 1b: C₂₈H₂₃N₂O₈Cl, m.p.: 202-204 °C; yield: 68%. R_f: 0.541; IR (KBr, ν_{\max} , cm^{-1}): 3442 (-OH *str.*); 1661 (C=O *str.*), 1740 (C=O *str.*), 701 (C-Cl *str.*), 1260 (N-N *str.*), 1610 (C=C *str.*), 2985 (-OCH₃ *str.*), 1122 (C-OC *str.*); 1197 (C-N *str.*); $^1\text{H NMR}$: δ 3.85 (s, 6H, Ar-O-CH₃), 11.9 (s, 1H, -OH), 6.9 (s, 1H, -CO-CH=C<), 4.40 (s, 2H, -OCH₂-), 6.5-7.9 (m, 10H, Ar-H), 8.92 (s, 1H, -CONH), 6.1 (s, 1H, -N-CH-ph), 4.60 (s, 1H, -CH-Cl). MS(EI, *m/z*): 551 (M+H⁺).

SLP VI 1c: C₂₈H₂₃N₃O₆Cl, m.p.: 185-187 °C; yield: 55%. R_f: 0.57; IR (KBr, ν_{\max} , cm^{-1}): 2985 (-OCH₃ *str.*), 1660 (C=O *str.*), 1615 (C=C *str.*), 1260 (N-N *str.*), 1740 (C=O *str.*), 1197 (C-N *str.*), 1122 (C-O-C *str.*), 694 (C-Cl *str.*); $^1\text{H NMR}$: δ 3.82 (s, 3H, Ar-O-CH₃), 3.14 (s, 6H, -N(CH₃)₂), 6.6 (s, 1H, -CO-CH=C<), 4.4 (s, 2H, -OCH₂-), 6.5-8.2 (m, 11H, Ar-H), 8.90 (s, 1H, -CONH), 5.92 (s, 1H, -N-CH-ph), 4.58 (s, 1H, -CH-Cl). MS(EI, *m/z*): 548 (M+H⁺).

SLP VI 1d: C₂₇H₁₉N₂O₆Cl₃, m.p.: 201-203 °C; yield: 64%. R_f: 0.616 (Benzene:acetone 7:3); IR (KBr, ν_{\max} , cm^{-1}): 2985.13 (-OCH₃ *str.*), 1742.11 (C=O *str.*), 1657.46 (C=O *str.*), 1616.87



(C=C *str.*), 1190.67 (C-N *str.*), 1120.45 (C-O-C *str.*), 1265.38 (N-N *str.*), 720-660 (C-Cl *str.*); ¹H NMR: δ 3.80 (s, 3H, Ar-O-CH₃), 6.92 (s, 1H, -CO-CH=C<), 4.43 (s, 2H, -OCH₂-), 6.5-7.9 (m, 10H, Ar-H), 8.90 (s, 1H, -CONH), 5.91 (s, 1H, -N-CH-ph), 4.42 (s, 1H, -CH-Cl). MS (EI, *m/z*): 574 (M+H⁺).

SLP VI 2a: C₂₉H₂₆N₃O₆Cl, m.p.: 189-191 °C; yield: 70%. R_f: 0.611; IR (KBr, ν_{max}, cm⁻¹): 2970 (-OCH₃ *str.*), 1744 (C=O *str.*), 1664 (C=O *str.*), 1605 (C=C *str.*), 1250 (N-N *str.*), 1200 (C-N *str.*), 1120 (C-O-C *str.*), 714 (C-Cl *str.*); ¹H NMR: δ 3.81 (s, 3H, Ar-O-CH₃), 3.14 (s, 6H, -N(CH₃)₂), 6.88 (s, 1H, -CO-CH=C<), 4.43 (s, 2H, -OCH₂-), 6.4-8.5 (m, 11H, Ar-H), 8.89 (s, 1H, -CONH), 6.02 (s, 1H, -N-CH-ph), 4.57 (s, 1H, -CH-Cl). MS (EI, *m/z*): 548 (M+H⁺).

SLP VI 2b: C₃₀H₂₈N₃O₇Cl, m.p.: 194-196 °C; yield: 64%. R_f: 0.603; IR (KBr, ν_{max}, cm⁻¹): 2970 (-OCH₃ *str.*), 1744 (C=O *str.*), 1664 (C=O *str.*), 1605 (C=C *str.*), 1250 (N-N *str.*), 1200 (C-N *str.*), 1120 (C-O-C *str.*), 714 (C-Cl *str.*); ¹H NMR: δ 3.81 (s, 6H, Ar-O-CH₃), 3.14 (s, 6H, -N(CH₃)₂), 6.9 (s, 1H, -CO-CH=C<), 4.43 (s, 2H, -OCH₂-), 6.4-8.2 (m, 10H, Ar-H), 8.89 (s, 1H, -CONH), 6.02 (s, 1H, -N-CH-ph), 4.58 (s, 1H, -CH-Cl). MS (EI, *m/z*): 578 (M+H⁺).

SLP VI 2c: C₃₀H₂₉N₄O₅Cl, m.p.: 176-178 °C; yield: 66%. R_f: 0.613; IR (KBr, ν_{max}, cm⁻¹): 1754 (C=O *str.*), 1662 (C=O *str.*), 1605 (C=C *str.*), 1250 (N-N *str.*), 1200 (C-N *str.*), 1120 (C-O-C *str.*), 711 (C-Cl *str.*); ¹H NMR: 2.98 (s, 12H, -N(CH₃)₂),

6.88 (s, 1H, -CO-CH=C<), 4.40 (s, 2H, -OCH₂-), 6.4-8.1 (m, 11H, Ar-H), 8.89 (s, 1H, -CONH), 6.02 (s, 1H, -N-CH-ph), 4.58 (s, 1H, -CH-Cl). MS (EI, *m/z*): 561 (M+H⁺).

SLP VI 2d: C₂₈H₂₂N₃O₅Cl₃, m.p.: 198-200 °C; yield: 61%. R_f: 0.636; IR (KBr, ν_{max}, cm⁻¹): 1740.63 (C=O *str.*), 1662.15 (C=O *str.*), 1611.52 (C=C *str.*), 1242.90 (N-N *str.*), 1220.41 (C-N *str.*), 1123.01 (C-O-C *str.*), 715.16-698.22 (C-Cl *str.*); ¹H NMR: 3.16 (s, 6H, -N(CH₃)₂), 6.79 (s, 1H, -CO-CH=C<), 4.41 (s, 2H, -OCH₂-), 6.2-8.2 (m, 10H, Ar-H), 8.72 (s, 1H, -CONH), 6.10 (s, 1H, -N-CH-ph), 4.52 (s, 1H, -CH-Cl). MS (EI, *m/z*): 586 (M+H⁺).

Biological evaluation

In vitro antioxidant activity

DPPH radical scavenging assay: The DPPH radical scavenging assay is based on the reduction of DPPH and stabilization of radical reactant. The change in colour from violet to yellow and the significant decrease in absorbance at 517 nm indicate increase in radical scavenging activity. The comparative radical scavenging activity of synthesized flavones [SLP II 1-2] and their azetidinone SLP VI [1(a-d)-2(a-d)] against 2,2-diphenyl-2-picryl hydrazyl hydrate (DPPH) was determined by using ascorbic acid as a standard [14].

% Radical scavenging activity was calculated by using the following equation:

$$\text{Inhibition (\%)} = \frac{AB - AS}{AB} \times 100$$

where, AB = absorbance of blank sample ($t = 0$ min); AS = absorbance of test sample. All the measurements were done in triplicate and results are presented as mean \pm SEM. A dose response curve was plotted to determine the IC₅₀ values.

Cardio protective activity

Animals and experimental protocol: The study was carried out on healthy wistar albino rats weighing between 180-230 g of male sex procured from Raghavendra enterprises, Bangalore, India. They were housed in clean propylene cages and allowed to acclimatize for 7 days before experimental use. They were maintained under standard conditions (25 ± 2 °C, relative humidity 44-56% and 12 h light and dark cycles, respectively). All the animals were maintained with free access for rat feed and purified drinking water ad libitum for 1 week before and during the experiment. The experimental protocol used in the present study was approved by Institutional Animal Ethical Committee (1423/PO/a/11/CPCSEA/104/2019).

The test compounds were selected based on the *in vitro* antioxidant assay among the newly synthesized title compounds. The potent antioxidant derivatives (**VI 1b**, **VI 1c**, **VI 2b** and **VI 2d**) were selected to evaluate cardio protective activity. The LD₅₀ values of the test compounds were determined on acute oral toxicity studies carried out as per OECD guidelines and were found to be 250 mg/kg body weight.

The experimental animals were randomly divided in to 7 different groups ($n = 6$) and treated as per the treatment schedule given. Group I and Group II were received a vehicle and termed as normal control and doxorubicin control respectively. Group III (Standard) received Vitamin-E 100 mg/kg [15]. Group IV, Group V, Group IV and Group VII test groups received 50 mg/kg of test compounds **VI 1b**, **VI 1c**, **VI 2b** and **VI 2d**, respectively as effective dose. All treatments were continued for 10 days by the oral route. Except for Group I, all the other six groups were subjected to doxorubicin toxicity with the dose of 15 mg/kg, i.p. on the 7th day [16-19].

Serum biochemical assay: After the experimental period, rats were anesthetized using diethyl ether by inhalation then the blood samples were collected from the retroorbital venous plexus of rats. After collecting the blood in eppendorf tubes containing sodium citrate, they were kept for 1 h at room temperature and serum was separated by centrifugation at 2000 rpm for 15 min and stored until analyzed for various biochemical parameters, creatine kinase-MB (CK-MB) [20], lactate dehydrogenase (LDH), serum glutamic oxaloacetic transaminase (SGOT), total cholesterol and triglycerides by using commercial kits with the help of semi-auto analyzer (Aruba).

Estimation of myocardial tissue parameters: After the blood samples were obtained, rats were killed by over anesthesia and hearts were removed rapidly. The tissues of heart were excised and washed with prechilled physical saline, homogenized with physical saline in tissue homogenizer and then centrifuged at 10,000 rpm for 10 min at 4 °C. The supernatants were assayed immediately for reduced glutathione (GSH) [21],

catalase (CAT) [22], superoxide dismutase (SOD) [23] and lipid peroxidation (LPO) [24].

Histopathological studies: For histopathological studies, myocardial tissue obtained from the excised heart was immediately fixed in 10% buffered neutral formalin solution. The fixed tissues were embedded in paraffin and serial sections were cut, stained with hematoxylin and eosin (H & E stain). The sections were examined under light microscope and photomicrographs were taken.

Statistical analysis: All the data was expressed as mean \pm SEM. Statistical significance between more than two groups was tested using one way ANOVA followed by the Tukey test using computer based fitting program (Prism graph pad 5.3). Statistical significance was set accordingly. Differences were considered to be statistically significant at $p < 0.05$.

Molecular docking: The crystal structures of the target-proteins MAPKinase P38 (PDB ID: 4DLI) and PKC β (PDB ID: 2IOE) were procured from Protein Data Bank. The synthesized test-ligands were separately docked at the ligand-binding sites of the corresponding target-proteins using Autodock 4.2 docking tools. The docked structures were visualized in BIOVIA Discovery Studio Visualizer 2019 [25] and the associated interaction energies were tabulated.

RESULTS AND DISCUSSION

Scheme-I illustrates the synthesis of flavones backbone (**SLP II 1-2**) and further synthesis of compounds of interest **SLP VI 1(a-d)–2(a-d)**. The chemical synthesis of flavones and their azetidinone tethered derivatives was commenced in accordance to synthetic procedure with optimum yields. The structures of these compounds were confirmed by IR, ¹H NMR and mass spectral data. 2,3-Unsaturation and 4-oxo functionality (flavones) raise the antioxidant potency than compounds lacking either of these features among flavonoids [26]. The 7-OH position on flavones was selected for tethering as it is most reactive -OH group even in natural flavones for glycosylation. The substituent at 3' and 4' positions on the ring B of flavone scaffold were chosen among those frequently found in naturally occurring compounds, such as methoxy (-OCH₃) and hydroxyl (-OH) groups. The literature revealed that the methylation of -OH decrease the antioxidant activity but it could improve the ADME of flavonoids [27]. Furthermore, Bak *et al.* [28] investigated and found that 4' N-substituted amino group promote free radical scavenging activity of different flavonoids. Therefore, the title compounds designed with substitution of -OCH₃ and -N(CH₃)₂ on flavones and -OCH₃, -OH and -N(CH₃)₂ aryl azetidinone at various positions.

In vitro antioxidant activity: In present study, the antioxidant property of the synthesized compounds was determined *in vitro* with DPPH assay method. The IC₅₀ values of all the screened compounds have been presented in Table-1. The comparative antioxidant effect of **SLP VI 1(a-d)–2(a-d)** with **SLP II (1-4)** indicated by Fig. 1.

The radical scavenging effect is associated with position and nature of substitution on flavone, 2-azetidinone moiety in tethered derivatives. As can be seen in Table-1, all the azetidinone tethered flavone compounds showed good antioxidant property

TABLE-1
ANTIOXIDANT ACTIVITY OF COMPOUNDS
SLP II (1-2) AND SLP VI 1(a-d)-2(a-d)

Compound	IC ₅₀ (µg/mL)	Compound	IC ₅₀ (µg/mL)
Ascorbic acid	16 ± 0.04	SLP VI 1d	52.6 ± 0.03
SLP II 1	42 ± 0.07	SLP VI 2a	41 ± 0.02
SLP II 2	47 ± 0.03	SLP VI 2b	35 ± 0.05
SLP VI 1a	40.2 ± 0.02	SLP VI 2c	54 ± 0.08
SLP VI 1b	32.1 ± 0.04	SLP VI 2d	39 ± 0.05
SLP VI 1c	36 ± 0.05		

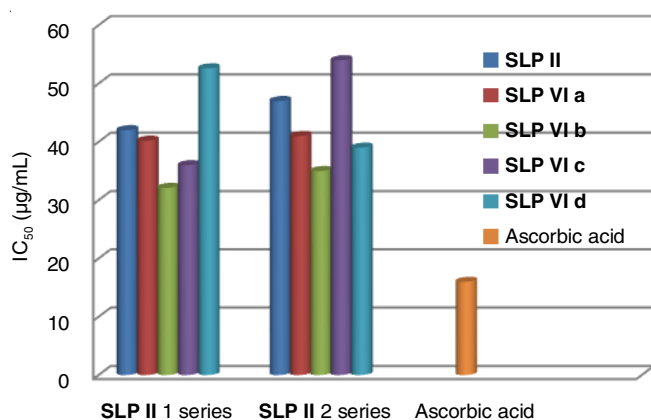


Fig. 1. Comparative antioxidant effect of SLP VI 1(a-d)-2(a-d) with SLP II (1-4)

especially SLP VI 1b, VI 1c, VI 2b and VI 2d have better reducing power in concentration range of 20-100 µg/mL with IC₅₀ 32.1 µg/mL, 36 µg/mL and 35 µg/mL, 39 µg/mL, respectively. The presence of electron donating substitution may be making them the better radical scavengers.

Cardioprotective effect

Effect of test compounds on serum biochemical parameters: Serum levels of cardiac marker enzymes such as CK-

MB, LDH ($p < 0.001$), transaminases such as SGOT ($p < 0.05$), total cholesterol ($p < 0.05$) and triglycerides ($p < 0.01$) were significantly higher in the doxorubicin control group as compared with the normal control group. Rats pretreated with test compounds VI 1b, VI 1c, VI 2b and VI 2d shows decreased levels of serum cardiac marker enzymes such as CK-MB ($p < 0.001$), LDH ($p < 0.01$), SGOT ($p < 0.05$), total cholesterol ($p < 0.05$) and triglycerides ($p < 0.05$) as compared with doxorubicin control group as shown in Table-2.

Effect of test compounds on oxidative parameters in heart tissue homogenate: Doxorubicin control group exhibited marked elevation in lipid peroxidation levels and reduction of endogenous catalase, glutathione and superoxide dismutase as compared to a normal control group. Marked reduction of doxorubicin-induced oxidative stress was observed with test compounds VI 1b, VI 1c, VI 2b, VI 2d, which was confirmed by significant reduction of LPO ($p < 0.01$) and significant elevation of CAT ($p < 0.05$), GSH ($p < 0.01$) and SOD ($p < 0.01$) as compared with doxorubicin control group. The changes of antioxidant parameters in cardiac tissue homogenate are shown in Table-3.

Effect of test compounds on histopathological examination of cardiac tissue: Effect of pre-treatment of test compounds VI 1b, VI 1c, VI 2b and VI 2d on doxorubicin-induced histopathological changes in rat cardiac tissue is depicted in Fig. 2. Histopathological studies of the normal control group of hearts showed normal myocardium structure. In doxorubicin intoxicated group of animals showed the necrotic changes in myocardial tissue along with hemorrhage. The standard group animals showed normal cytoarchitecture of myocardium. Pre-treatment with test compounds VI 1c, VI 2b rats showed regenerative changes in myocardial tissue. The morphology of cardiac muscle was relatively preserved and showed similar characteristic features with normal group in rats treated with test compounds VI 1b and VI 2d.

TABLE-2
EFFECT OF TEST COMPOUNDS ON DOXORUBICIN INDUCED ALTERATIONS ON SERUM BIOCHEMICAL PARAMETERS

Group	CK-MB (IU/L)	LDH (IU/L)	SGOT (IU/L)	Total cholesterol (mg/dL)	Triglycerides (mg/dL)
Normal control	130.5 ± 3.28	188.5 ± 7.227	35.53 ± 2.51	21.35 ± 1.63	27.56 ± 1.32
Doxorubicin control	343.2 ± 12.72a	759.2 ± 26.46 a	103.5 ± 5.34 c	45.10 ± 8.24 c	65.75 ± 4.14 b
Test 1 (VI 1b)	239.8 ± 5.21 a	659.1 ± 19.21 b	67.29 ± 7.27 c	22.14 ± 1.19 c	38.64 ± 3.16 c
Test 2 (VI 1c)	237.3 ± 6.11 a	661.3 ± 14.72 b	65.27 ± 6.28 c	20.54 ± 0.63 c	40.28 ± 6.41 c
Test 3 (VI 2b)	256.4 ± 4.23 a	622.8 ± 17.66 b	71.09 ± 4.22 c	20.74 ± 3.49 c	41.68 ± 3.08 c
Test 4 (VI 2d)	261.3 ± 8.22 a	647.2 ± 18.31 b	68.39 ± 6.21 c	28.34 ± 2.69 c	40.66 ± 2.36 c
Standard	178.9 ± 4.80 a	365.3 ± 12.55 a	63.26 ± 5.23 c	18.99 ± 1.65 c	22.47 ± 1.02 b

All values are presented as mean ± SEM (n = 6). $p < 0.001$ is denoted by a, $p < 0.01$ is denoted by b and $p < 0.05$ is denoted by c.

TABLE-3
EFFECT OF TEST COMPOUNDS ON CARDIAC TISSUE ENDOGENOUS ANTIOXIDANT SYSTEMS

Group	SOD (U/mg protein)	CAT (µmol H ₂ O ₂ decomposed mg protein/min)	GSH (nmol of GSH/mg protein)	LPO (nmol of MDA/mg protein)
Normal control	22.52 ± 0.37	20.98 ± 2.08	17.99 ± 0.94	9.02 ± 0.59
Doxorubicin control	9.69 ± 1.03 b	7.17 ± 0.4 c	5.19 ± 1.57 b	32.90 ± 2.36 b
Test 1 (VI 1b)	17.21 ± 1.16 b	18.53 ± 0.59 c	11.02 ± 1.07 b	15.12 ± 0.56b
Test 2 (VI 1c)	20.37 ± 1.58 b	18.51 ± 0.44 c	13.55 ± 0.52 b	17.62 ± 0.41b
Test 3 (VI 2b)	17.58 ± 3.21 b	20.13 ± 2.48c	14.03 ± 0.39 b	12.33 ± 0.93b
Test 4 (VI 2d)	19.33 ± 1.03 b	17.73 ± 2.59 c	13.98 ± 0.51 b	17.85 ± 1.21b
Standard	21.85 ± 1.81 c	27.69 ± 2.38 b	22.23 ± 0.92 a	11.66 ± 0.48 b

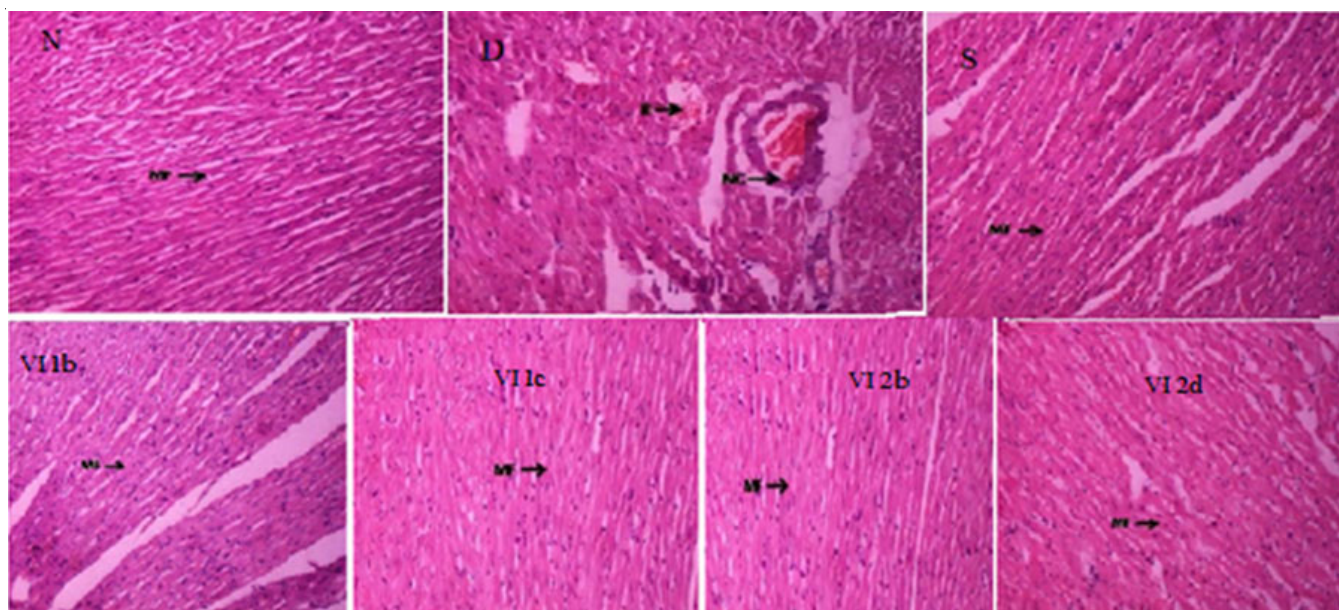


Fig. 2. Effect of doxorubicin induced cardiotoxicity on histopathological alterations and its amelioration by test compounds in rat hearts. N. Normal control; D. Doxorubicin control; S. Standard; Test compounds VI 1b, VI 1c, VI 2b, VI 2d. H-Haemorrhage, MF-Myocardial fibres

Docking studies: The docking results were tabulated in Table-4. The interaction energies of synthesized flavones **SLP II 1** and its corresponding azetidinone tethered derivatives **SLP VIIa**, **VI 1b**, **VI 1c** and **VI 1d** with MAP Kinase P38 were -8.32, -8.16, -9.67, -10.37 and -8.90 kcal/mol, respectively.

The structure of **SLP II 1** ligand docked with MAPk P38 at its ligand binding site illustrated that it interacts with Leu-291, Ser-293 residues through hydrogen bonds and with Leu-246, Trp-197, Ser-252, Asn-196, Leu-195 and Ala-255 residues of the protein through π - π stacked, amide- π stacked and other interactions (Fig. 3b and c).

Among the azetidinone tethered derivatives **SLPVI 1c** has highest binding energy compared to **SLP II 1**. The structure of **SLPVI 1c** ligand docked with MAPk P38 at its ligand binding site illustrated that it interacts with Leu-195, Ser-251, Ser-252 and Ser-254 residues through conventional hydrogen bonds and with Leu-246, Leu-291, Glu-192, Ileu-250, Ala-255, Asn-

Ligand	Interaction energies with MAPKinaseP38 (Kcal/mol) [PDB id: 4DLI]	Interaction energies with PKC β (Kcal/mol) [PDB id:2IOE]
SLP II 1	-8.32	-7.79
SLP VI 1a	-8.16	-7.07
SLP VI 1b	-9.67	-7.94
SLP VI 1c	-10.37	-8.72
SLP VI 1d	-8.90	-8.50
SLP II 2	-8.28	-7.48
SLP VI 2a	-10.7	-7.67
SLP VI 2b	-8.28	-9.48
SLP VI 2c	-9.14	-8.79
SLP VI 2d	-7.55	-8.34

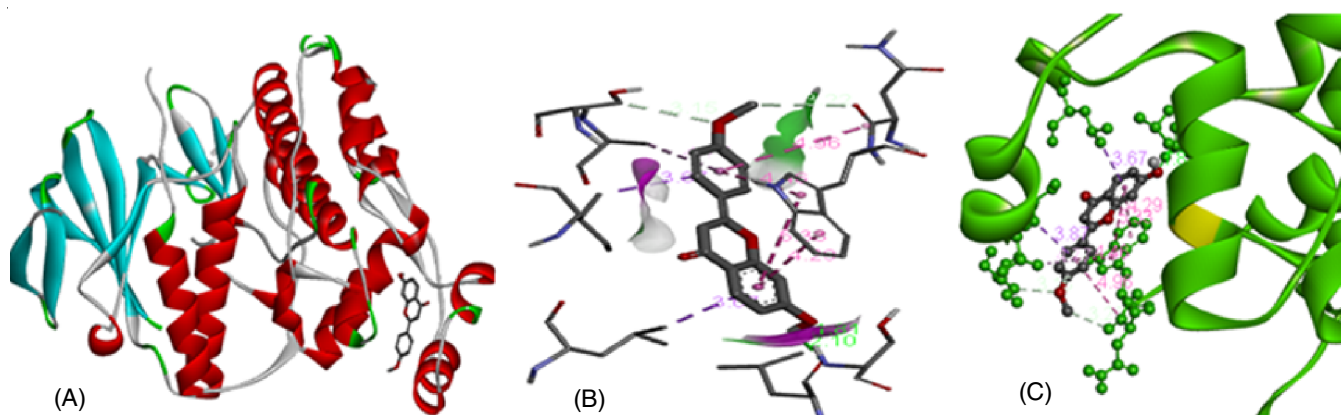


Fig. 3. 3D illustrations of interactions of **SLP III** (A) receptor interaction (B) hydrogen bonding surface (C) interactions with pocket atoms of corresponding amino-acid residues of MAP kinase P38. Autodock 4.2 and Biovia discovery studio2019 Viewer were used to generate and visualize the docked structures respectively

196 and Trp-197 residues of the protein through π - π stacked, Amide- π stacked and other interactions (Fig. 4b and c).

The interaction energies of synthesized flavones **SLP II 2** and its corresponding azetidinone tethered derivatives **SLP VI2a**, **VI2b**, **VI2c** and **VI2d** with MAPKinase P38 were -8.28, -10.7, -8.28, -9.14 and -7.55 kcal/mol respectively. The structure of compound **SLP II 2** ligand docked with MAPk P38 at its ligand binding site illustrated that it interacts with Asp-292 residue through hydrogen bond and with Leu-195, Ser-251, Asn-196, Ile-250, Ala-255, Glu-192, Leu-246 and Trp-197 residues of the protein through Pi-sigma, π - π stacked, amide- π stacked and other interactions (Fig. 5b and c).

Among the azetidinone tethered derivatives **SLP VI 2a** has highest binding energy compared to compound **SLP II 2**. The structure of compound **SLP VI2a** ligand docked with MAPk P38 at its ligand binding site illustrated that it interacts with Arg-23 residue through conventional hydrogen bond and with Lys-76, Val-349, Lys-79, Leu-87, Leu-353, Thr-46 and Pro-351 residues of the protein through other interactions (Fig. 6b and c).

The interaction energies of synthesized flavones **SLP II 1** and its corresponding azetidinone tethered derivatives **SLP VIIa**, **VIIb**, **VIIc** and **VIIc** with PKC β were -7.79, -7.07, -7.94, -8.72 and -8.50 kcal/mol, respectively. The structure of

compound **SLP II 1** ligand docked with PKC β at its ligand binding site illustrated that it interacts with Lys-399, Leu-406 and Ala-395 residues through hydrogen bonds and with Gln-405, Leu-396 and Pro-397 residues of the protein through Pi-lonepair, Pi-alkyl and other interactions (Fig. 7b and c).

Among the azetidinone tethered derivatives **SLPVI 1c** has highest binding energy compared to compound **SLP II 1**. The structure of compound **SLPVI 1c** ligand docked with PKC β at its ligand binding site illustrated that it interacts with Lys-399, Leu-406 and Ser-664 residues through conventional hydrogen bonds and with Ala-395, Asn-663 and Phe-661 residues of the protein through Pi-lone pair and other interactions (Fig. 8b and c).

The interaction energies of synthesized flavones **SLP II 2** and its corresponding azetidinone tethered derivatives **SLP VI2a**, **VI2b**, **VI2c** and **VI2d** with PKC β were -7.48, -7.67, -9.48, -8.79 and -8.34 kcal/mol, respectively. The structure of compound **SLP II 2** ligand docked with PKC β at its ligand binding site illustrated that it interacts with Tyr-422, Glu-366 and Tyr-368 residue through hydrogen bond and with Arg-624, Leu-367, Lys-668 and Pro-669 residues of the protein through Pi-sigma, Pi-alkyl and other interactions (Fig. 9b and c).

Among the azetidinone tethered derivatives **SLP VI 2b** has highest binding energy compared to compound **SLP II 2**.

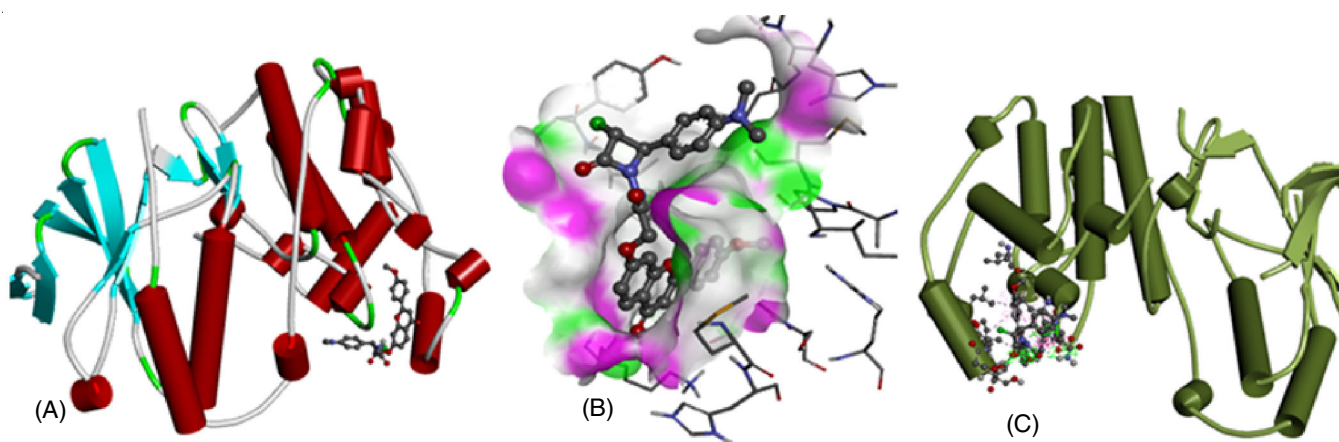


Fig. 4. 3D illustrations of interactions of **SLP VI 1C** (A) receptor interaction (B) hydrogen bonding surface (C) interactions with pocket atoms of corresponding amino-acid residues of MAP kinase P38. Autodock 4.2 and Biovia discovery studio2019 Viewer were used to generate and visualize the docked structures respectively

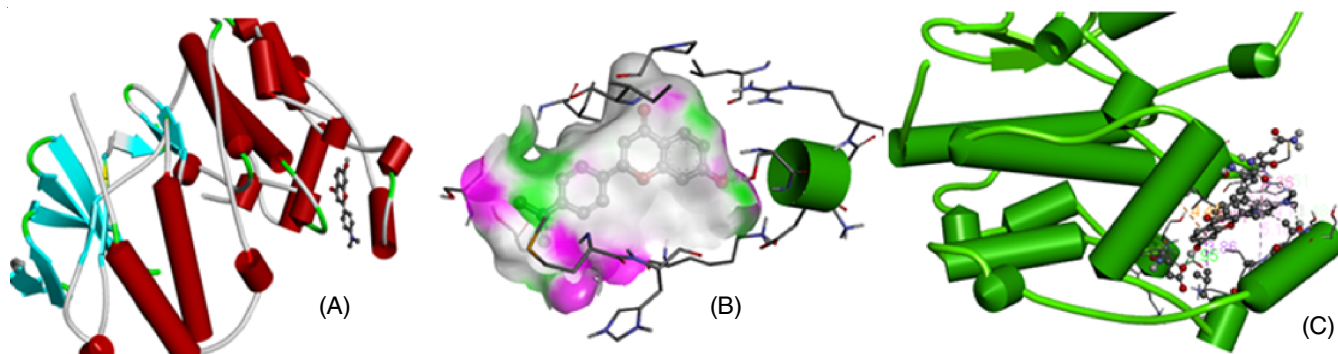


Fig. 5. 3D illustrations of interactions of **SLP II 2** (A) receptor interaction (B) hydrogen bonding surface (C) interactions with pocket atoms of corresponding amino-acid residues of MAP kinase P38. Autodock 4.2 and Biovia discovery studio2019 Viewer were used to generate and visualize the docked structures respectively

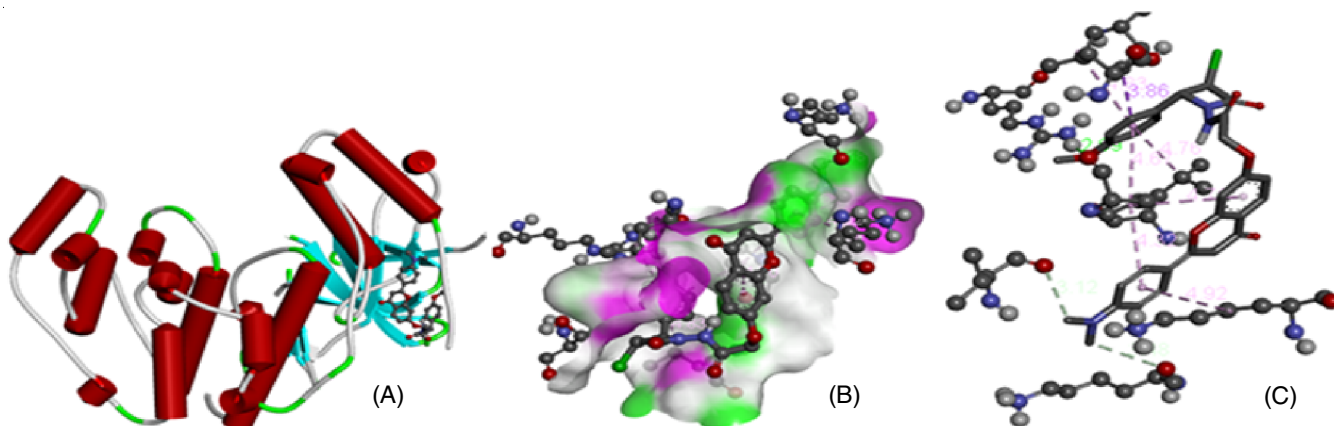


Fig. 6. 3D illustrations of interactions of **SLP VI2d** (A) receptor interaction (B) hydrogen bonding surface (C) interactions with pocket atoms of corresponding amino-acid residues of MAP kinase P38. Autodock 4.2 and Biovia discovery studio2019 Viewer were used to generate and visualize the docked structures respectively

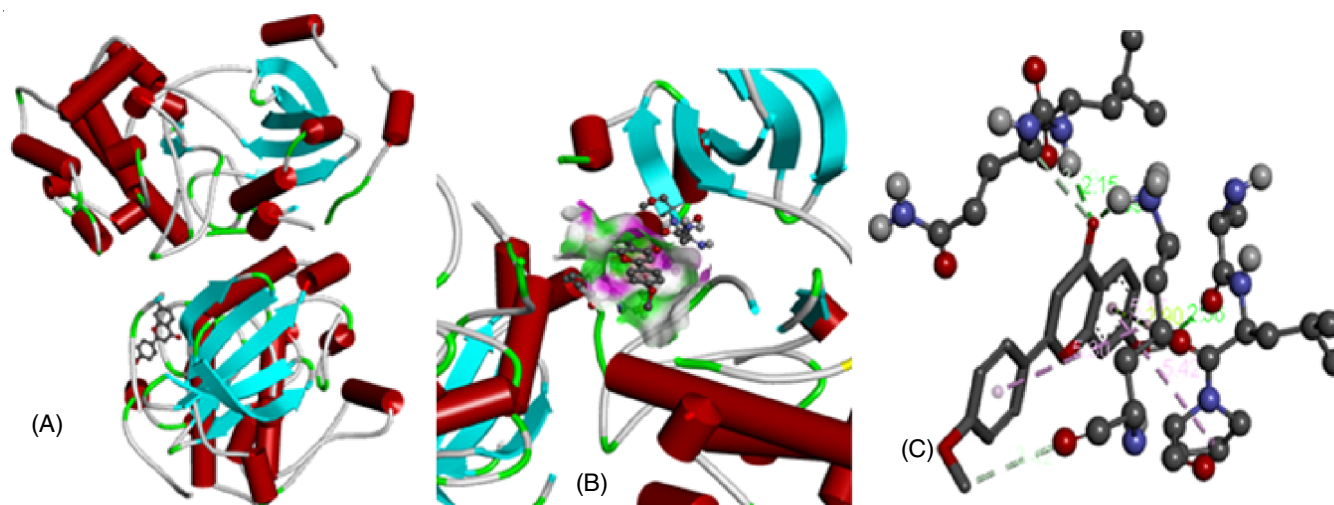


Fig. 7. 3D illustrations of interactions of **SLP III1** (A) receptor interaction (B) hydrogen bonding surface (C) interactions with pocket atoms of corresponding amino-acid residues of PKC β . Autodock 4.2 and Biovia discovery studio2019 Viewer were used to generate and visualize the docked structures respectively

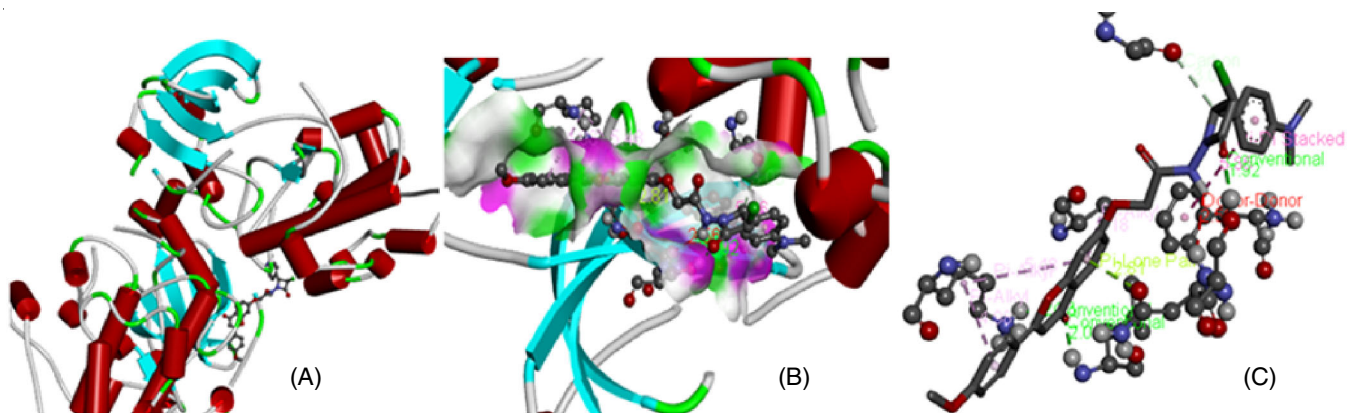


Fig. 8. 3D illustrations of interactions of **SLP VI 1c** (A) receptor interaction (B) hydrogen bonding surface (C) interactions with pocket atoms of corresponding amino-acid residues of PKC β . Autodock 4.2 and Biovia discovery studio2019 Viewer were used to generate and visualize the docked structures respectively

The structure of compound **SLP VI2b** ligand docked with PKC β at its ligand binding site illustrated that it interacts with Leu-403, Lys-399 residue through conventional hydrogen

bond, with Lys-611 Pi-cation, Leu-667 Pi-sigma, with Glu-665, Leu-396, Gly-398, Pro-400, Pro-401, Arg-610 residues of the protein through other interactions (Fig. 10b and c).

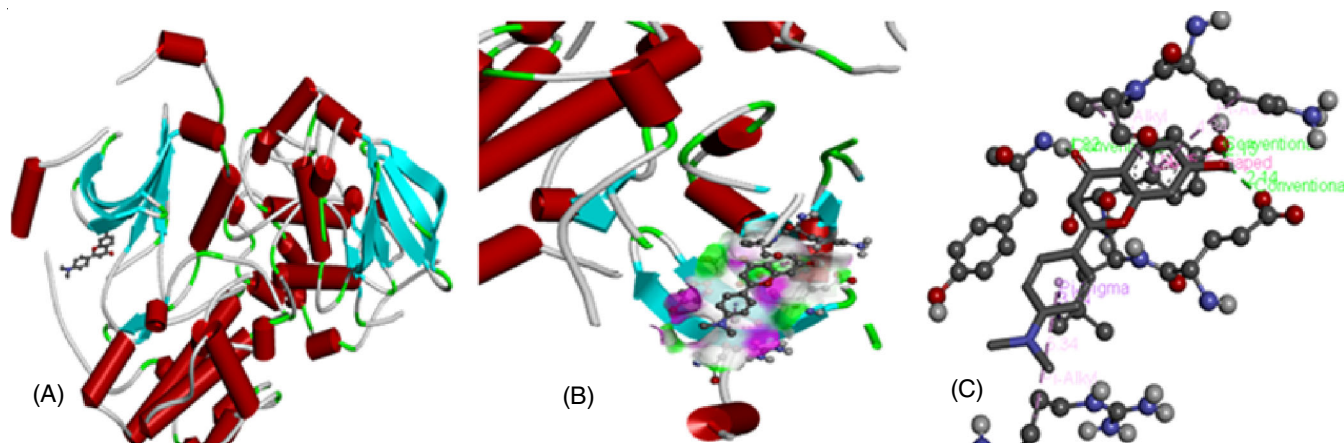


Fig. 9. 3D illustrations of interactions of **SLP II2** (A) receptor interaction (B) hydrogen bonding surface (C) interactions with pocket atoms of corresponding amino-acid residues of PKC β . Autodock 4.2 and Biovia discovery studio2019 Viewer were used to generate and visualize the docked structures respectively

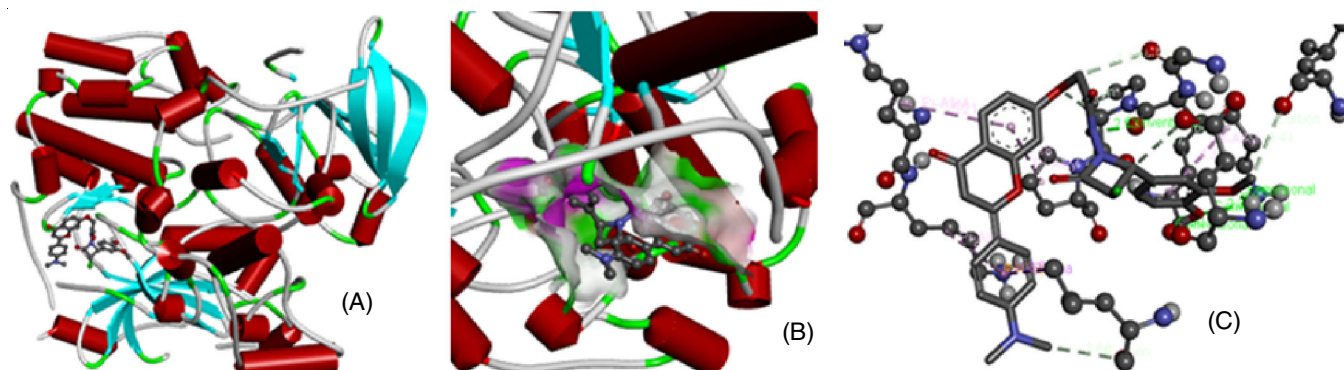


Fig. 10. 3D illustrations of interactions of **SLP VI2d** (A) receptor interaction (B) hydrogen bonding surface (C) interactions with pocket atoms of corresponding amino-acid residues of PKC β . Autodock 4.2 and Biovia discovery studio2019 Viewer were used to generate and visualize the docked structures respectively

The results of molecular docking carried-out in current study revealed that the azetidinone tethered derivatives have good binding energies compared to their precursor flavone molecules **SLP III 1** and **SLP II 2**. They have good binding affinity towards MAPK P38 target protein than PKC β target comparitavly. Among all the derivatives **SLPVI1c** and **SLP VI2b** have high binding energies to both cardioprotective target proteins [29] MAPK P38 and PKC β .

Conclusion

In conclusion, eight derivatives of 2-azetidinone tethered 4'-OCH₃ flavones and 4'-N(CH₃)₂ flavones were synthesized, characterized and evaluated for biological activity. According to the results the synthesized compounds had effective antioxidant activity. The data suggest that azetidinone tethered flavones [**SLP VI 1(a-d)**–**2(a-d)**] have moderately more antioxidant property compare to the synthesized flavone precursors [**SLP II 1-2**]. Compounds **SLPVI 1b**, **VI 1c**, **VI 2b** and **VI 2d** have high antioxidant property among the compounds tested and further evaluated for cardioprotective effect. Compounds **VI 1b**, **VI 1c**, **VI 2b** and **VI 2d** significantly attenuated the levels of pathological biochemical markers like creatine kinase-MB (CK-MB), lactate dehydrogenase (LDH), serum glutamic oxaloacetic transaminase (SGOT), total cholesterol, triglyce-

rides and significantly raises the levels of endogenous protective antioxidant proteins in the doxorubicin-intoxicated rats. The docking studies on the test compounds revealed that they have high binding affinity to the MAP kinase P38 and PKC β target proteins. Based on the results, the research finding supports that the novel synthetic flavones derivatives have antioxidant and cardioprotective activity.

ACKNOWLEDGEMENTS

The authors are thankful to the management of Saraswathi Educational Society, Utukur, Kadapa, India for their support and providing the necessary research facilities for carrying out the work.

CONFLICT OF INTEREST

The authors declare that there is no conflict of interests regarding the publication of this article.

REFERENCES

1. P.D. Ray, P.W. Huang and Y. Tsuji, *Cell. Signal.*, **24**, 981 (2012); <https://doi.org/10.1016/j.cellsig.2012.01.008>
2. P. Shanmugam, A. Valente, S. Prabhu, B. Venkatesan, T. Yoshida, P. Delafontaine and B. Chandrasekar, *J. Mol. Cell. Cardiol.*, **50**, 928 (2011); <https://doi.org/10.1016/j.yjmcc.2011.02.012>

3. A.K. Dhalla, M.F. Hill and P.K. Singal, *J. Am. Coll. Cardiol.*, **28**, 506 (1996);
[https://doi.org/10.1016/0735-1097\(96\)00140-4](https://doi.org/10.1016/0735-1097(96)00140-4)
4. B.Y. Kang and J.L. Mehta, *J. Cardiovasc. Pharmacol. Ther.*, **14**, 283 (2009);
<https://doi.org/10.1177/1074248409344329>
5. P.C. Schenkel, A.M. Tavares, R.O. Fernandes, M. Bertagnolli, G.P. Diniz, A.S. da Rosa Araujo, M.L. Barreto-Chaves, M.F.M. Ribeiro, N. Clausell and A. Belló-Klein, *Mol. Cell. Biochem.*, **341**, 1 (2010);
<https://doi.org/10.1007/s11010-010-0431-8>
6. K. Koga, A. Kenessey, S. Powell, C.P. Sison, E.J. Miller and K. Ojamaa, *Antioxid. Redox Signal.*, **14**, 1191 (2011);
<https://doi.org/10.1089/ars.2010.3163>
7. G.M. Cragg, D.J. Newman and K.M. Snader, *J. Nat. Prod.*, **60**, 52 (1997);
<https://doi.org/10.1021/np9604893>
8. Z.L. Fowler, K. Shah, J.C. Panepinto, A. Jacobs and M.A.G. Koffas, *PLoS One*, **6**, e25681 (2011);
<https://doi.org/10.1371/journal.pone.0025681>
9. Z. Shutenko, Y. Henry, E. Pinar, J. Seylaz, P. Potier, F. Berthet, P. Girard and R. Sercombe, *Biochem. Pharmacol.*, **57**, 199 (1999);
[https://doi.org/10.1016/S0006-2952\(98\)00296-2](https://doi.org/10.1016/S0006-2952(98)00296-2)
10. A.R. Saundane, V. Katkar, A.V. Vajjinath and W. Prabhaker, *Med. Chem. Res.*, **22**, 806 (2013);
<https://doi.org/10.1007/s00044-012-0066-2>
11. D.S. Salunkhe and P.B. Piste, *Int. J. Pharm. Sci. Res.*, **5**, 666 (2014).
12. C. Amutha, S. Saravanan and S. Muthusubramanian, *Indian J. Chem.*, **53B**, 377 (2014).
13. P. Kohli, S.D. Srivastava and S.K. Srivastava, *J. Indian Chem. Soc.*, **85**, 326 (2008).
14. M. Éaëic, M. Molnar, B. Šarkanj, E. Has-Schön and V. Rajkovic, *Molecules*, **15**, 6795 (2010);
<https://doi.org/10.3390/molecules15106795>
15. A. Upaganlawar, C. Gandhi and R. Balaraman, *Plant Foods Hum. Nutr.*, **64**, 75 (2009);
<https://doi.org/10.1007/s11130-008-0105-9>
16. M.N. Nagi and M.A. Mansour, *Pharmacol. Res.*, **41**, 283 (2000);
<https://doi.org/10.1006/phrs.1999.0585>
17. S. Tabassum, K. Gangarapu, G. Thumma, S. Manda and R.N. Reddy Anreddy, *J. Chem.*, **2014**, 260672 (2014);
<https://doi.org/10.1155/2014/260672>
18. A.R.N. Reddy, J. Nagaraju, G. Rajyalaksmi and M. Sarangapani, *Toxicol. Environ. Chem.*, **94**, 2012 (2012);
<https://doi.org/10.1080/02772248.2012.741335>
19. M. Panteghini, F. Ceriotti, G. Schumann and L. Siekmann, *Clin. Chem. Lab. Med.*, **39**, 795 (2001);
<https://doi.org/10.1515/CCLM.2001.131>
20. B. Pradeepkumar, A. Sudheer, T. Srinath Reddy, K.S. Reddy, G. Narayana and K. Veerabhadrapa, *J. Young Pharm.*, **10**, 422 (2018);
<https://doi.org/10.5530/jyp.2018.10.93>
21. H. Aebi, *Enzymology*, **105**, 121 (1984);
[https://doi.org/10.1016/S0076-6879\(84\)05016-3](https://doi.org/10.1016/S0076-6879(84)05016-3)
22. H.P. Misra and I. Fridovich, *Arch. Biochem. Biophys.*, **181**, 308 (1977);
[https://doi.org/10.1016/0003-9861\(77\)90509-4](https://doi.org/10.1016/0003-9861(77)90509-4)
23. H. Ohkawa, N. Ohishi and K. Yagi, *Anal. Biochem.*, **95**, 351 (1979);
[https://doi.org/10.1016/0003-2697\(79\)90738-3](https://doi.org/10.1016/0003-2697(79)90738-3)
24. Dassault Systemes BIOVIA Discovery Studio Modeling Environment, Accelrys Software Inc., San Diego, USA (2017).
25. S. Kumar and A.K. Pandey, *Scientific World J.*, **2013**, 162750 (2013);
<https://doi.org/10.1155/2013/162750>
26. G. Cao, E. Soc and R.L. Prior, *Free Radic. Biol. Med.*, **22**, 749 (1997);
[https://doi.org/10.1016/S0891-5849\(96\)00351-6](https://doi.org/10.1016/S0891-5849(96)00351-6)
27. X. Wen and T. Walle, *Drug Metab. Dispos.*, **34**, 1786 (2006);
<https://doi.org/10.1124/dmd.106.011122>
28. P. Szabados-Furjesi, D. Pajtas, A. Barta, E. Csepanyi, A. Kiss-Szikszai, A. Tosaki and I. Bak, *Molecules*, **23**, 3161 (2018);
<https://doi.org/10.3390/molecules23123161>
29. R. Ravindran, S. Kumar, J. Rajkumar, S. Roy, S. Sathiya, C. Saravana Babu and M.J. Equbal, *Biol. Med. (Aligarh)*, **10**, 442 (2018);
<https://doi.org/10.4172/0974-8369.1000442>